Romanian Reports in Physics, Vol. 67, No. 4, P. 1457–1466, 2015

Dedicated to
International Year of Light 2015

PHOTOPHYSICS OF COVALENT FUNCTIONALIZED SINGLE WALLED CARBON NANOTUBES WITH A PORPHYRIN-TYPE PHOTOSENSITIZER

ANGELA STAICU[1, *], A. PASCU[1], V. NASTASA[1,2], M.L. PASCU[1,2]

[1] National Institute for Lasers, Plasma and Radiation Physics, Laser Department, 409 Atomistilor St., RO-077125, Magurele, Ilfov, Romania
E-mails: angela.staicu@inflpr.ro, alex. pascu@inflpr.ro, viorel.nastasa@inflpr.ro, mihai.pascu@inflpr.ro
[2] University of Bucharest, Faculty of Physics, RO-077125, Magurele, Ilfov, Romania
[*] Author for correspondence: angela.staicu@inflpr.ro

Received October 8, 2015

Abstract. We report photophysics studies of some compounds of interest in drug targeted delivery and conjugated single walled carbon nanotubes with a photosensitizing agent. Supramolecular entities porphyrin-carbon nanotubes have been synthesized by covalent functionalization and have been analyzed in terms of photostability, microfluidics (surface tension and viscosity) and laser induced fluorescence properties. Likewise, their chemical bonding structure was studied by FTIR spectroscopy. There were highlighted the photophysical characteristics of conjugated compounds with respect to the correspondent mixture of the raw components.

Key words: photophysics, microfluidics, single walled carbon nanotubes, porphyrin.

1. INTRODUCTION

Alternatives to synthesize new drugs, which became lately of outmost importance and should be considered in order to solve/treat the multiple drug resistance and side effects, are the development of targeted delivery systems for clinical approved drugs. The development of methods and mechanisms for controlled release of the drug at the right site is an actual task, as well. Novel therapy drugs imply their targeted delivery and intracellular activation. Potential tools for carrying the drugs/biomarkers to the targeted cells can be emulsions [1], foams [2, 3], vesicles, nanomaterials, etc. Single-walled carbon nanotubes (SWCNT) have been explored as novel drug delivery vehicles [4–8], since they are an unique quasi one-dimension material with light structure, having capacity to cross biological barriers (cells membranes). The combination of drugs and laser radiation has a promising potential in photo-therapy [9, 10], and finds applications in developments of new antibacterial compounds [11–20].

Here, we report the study of the photophysics of some compounds of interest in drug targeted delivery, conjugated SWCNT with a photosensitizing agent. Consequently, supramolecular entities porphyrin-carbon nanotubes have been synthesized by covalent functionalization and have been analyzed in terms of photostability, microfluidics (surface tension and viscosity), and Laser Induced Fluorescence (LIF) properties. Their chemical bonding structure was studied, too, by FTIR spectroscopy.

2. MATERIALS AND METHODS

The materials, equipment and experimental set-up used for chemical synthesis of the complex structure around the SWCNT as well as for their photophysical study are described in the following.

Chemical compounds and solvents: Amino-functionalized Single Walled Carbon Nanotubes purchased from Nanocs Inc. (Ø = 0.7–1.2 nm, bundle diameter ~ 20 nm, fiber length 20–50 μm, amino moiety to ends 0.25 to 0.45 mmol/g nanotubes); 5-mono (4-carboxyphenyl) -10,15,20-triphenyl porphine (TPP) from Frontier Scientific; N, N'-dicyclohexylcarbodiimide (DCC) from Merck; N, N-dimethylformamide (DMF) from Merck.

Amino functionalized nanotubes were conjugated with the porphyrinic molecules TPP (Fig. 1) using a carboxylation method that implies the activation and interaction of a carboxylic moiety with an amino group and has as result an amide bond.

SWCNT- NH2 TPP

Fig. 1 – The chemical structure of raw compounds.

The synthesis was performed according to the procedure introduced in [21]. Briefly, DCC was added to a porphyrin prepared in DMF solution; DCC has a catalytic role in the conversion of the -COOH group into an active ester group. In a second step, the SWCNT were added and mixed under nitrogen atmosphere for 48 hours.

In order to highlight the photophysics features of the synthesized product (noted *linked*), the measured descriptors (absorption, surface tension, fluorescence,

etc.) of it were compared with those of correspondent mixture of the raw components (noted *mixed*).

Steady-state absorption measurements of the samples were carried out using a Lambda 950 UV/Vis/NIR Spectrometer (Perkin Elmer). The photo-stability of the synthesized compounds was studied by irradiating the samples with the CW-radiation emitted by a Xe lamp and tailored by lenses and filters to obtain a beam power density of 145 mW/cm^2 in the 400 nm–800 nm spectral range. The comparative analysis of the absorption spectra of the irradiated and non-irradiated samples pointed out the photo-stability behavior of the irradiated samples.

The experimental set-up used for LIF measurements (Fig. 2) is described in details elsewhere [22]. It contains a pulsed Nd:YAG laser (Surelite II, Continuum, Excel Technology) frequency doubled to 532 nm, emitting pulses of 6 ns pulse time width at half maximum at 10Hz and used to excite the TPP molecules. The fluorescence signal was detected and analyzed using a system Spectrograph-ICCD Camera (Acton Research / Princeton Instruments). The spectrograph is a Spectra Pro type SP-2750 and camera, ICCD-PIMAX 1024 RB.

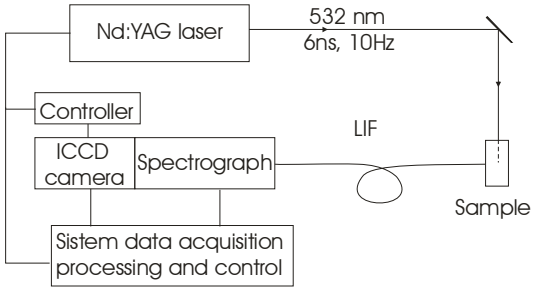

Fig. 2 – The LIF experimental set-up.

For the IR absorption study of the samples, it was used a FTIR spectrometer model Nicolet iS50, resolution 4 cm^{-1}. In this case, the samples were dried on the surface of optical grade KRS-5 plates and the resulting film has been then analyzed in the IR range between 4000 and 400 cm^{-1}. In order to demonstrate the formation of conjugates between the SWCNT and the porphyrin compound, the IR spectra of the *linked* samples were compared with the spectra of the constitutive compounds.

3. RESULTS AND DISCUSSIONS

3.1. ABSORPTION AND PHOTOSTABILITY STUDIES

As mentioned above, a comparative study of the optical absorption of the synthesized *linked* compound and of the *mixed* components (SWCNT and TPP) was carried out.

In Fig. 3 are shown the absorption spectra for the dispersions in DMF of the *linked* compounds and respectively of *mixed* ones, as well as for TPP in DMF at 2×10^{-7} M. The concentration of carbon nanotubes was 0.25 mg/ml. The TPP concentration in the mixture was chosen to fit the absorbance of the *linked* product with calibrated TPP samples. As for the *linked* structure, the main absorption band of TPP at 420 nm in the visible is well identified in its spectrum, proving the presence of TPP in the synthesized compound.

The photostability of the compounds was investigated by irradiating 60 minutes the samples in the visible between 400 nm and 800 nm with a beam having a power density of 145 mW/cm^2.

In Fig. 4a the absorption spectra are shown for *linked* un-irradiated and respectively irradiated samples, while in Fig. 4b the spectra of un-irradiated and irradiated *mixed* compounds in DMF are shown. The nanotubes concentration was 0.25 mg/ml and the TPP concentration was 2×10^{-7} M.

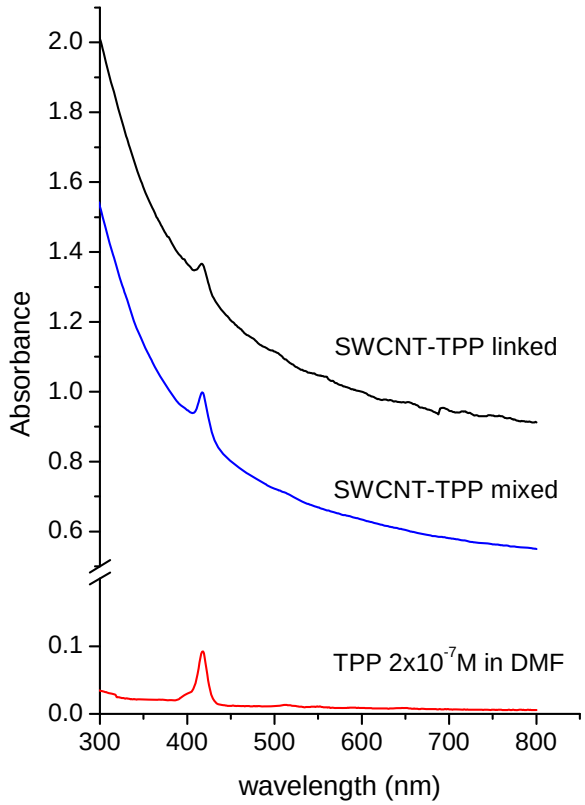

Fig. 3 – Absorption spectra of the studied compounds in DMF solutions (online color).

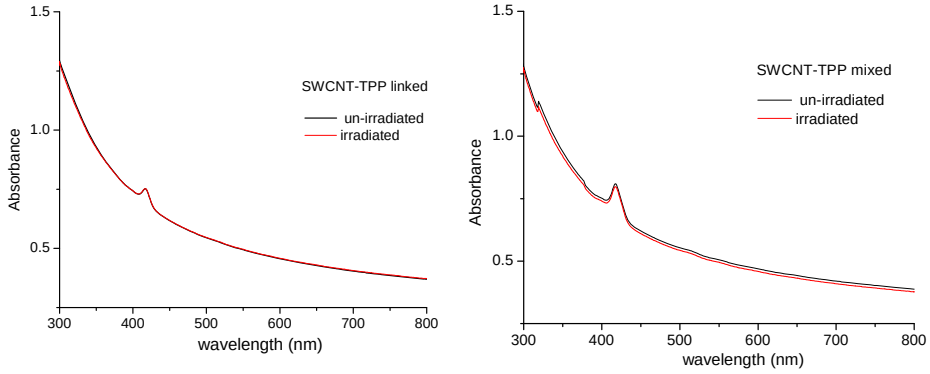

Fig. 4 – The absorption spectra for un-irradiated/irradiated samples: a) SWCNT-TPP linked, b) SWCNT-TPP mixed (online color).

It is obvious that the absorption spectra do not show changes after irradiation, proving in such way the photostability of the *linked* products.

3.2. MICROFLUIDIC PROPERTIES MEASUREMENTS: SURFACE TENSION AND VISCOSITY

Surface tension and viscosity measurements were performed with a PAT1 (Profile Analysis Tensiometer) from Sinterface (DE) which is analyzing a pendant droplet profile. This analysis is based on the Young Laplace equation that uses the fitted profile of the droplet to calculate the value of surface tension [23]. The equipment used for these measurements can maintain constant the droplet volume which fact eliminates the effects induced by liquid evaporation that could affect the measurements.

Table 1 shows the equilibrium surface tension values of DMF and DMF with nanotubes (SWCNT-TPP *linked* si SWCNT-TPP *mixed*). One can observe that the surface tension values are slightly influenced by the presence of carbon nanotubes in solutions.

Table 1

Solution	**ST (mN/m)**
DMF	37.8 ± 0.3
SWCNT-TPP linked	38.4 ± 0.2
SWCNT-TPP mixed	36.2 ± 0.4

In order to evaluate the rheological properties of the samples, a surface tension measurement was followed by a "surface disturbance-relaxation experiment" similar to that reported in [24] that consists in harmonic perturbations

induced to the pendant droplet followed by Fourier analysis of the obtained data. The droplet volume was varied with ±1 mm^3 and the frequencies used were 0.005, 0.008, 0.01, 0.02, 0.04, 0.05, 0.08, 0.1, 0.16 and 0.2 Hz.

The data obtained after the Fourier analysis of the harmonic perturbation measurements are in accordance with the surface tension results.

Figure 5 shows (a) the visco-elastic modulus (|*E*|) and (b) the phase lag (Φ) values for the studies compounds. These values were calculated from the E_{Im} si E_{Re} obtained from the Fourier analysis of the rheological data generated by the induced harmonic perturbations.

$$|E| = \sqrt{E_{re}^2 + E_{im}^2} = \frac{\Delta\sigma_m}{\frac{\Delta A_m}{A_0}} \tag{1}$$

$$\begin{aligned} E_{\mathrm{Re}} &= |E| \cdot \cos\phi, \\ E_{\mathrm{Im}} &= |E| \cdot \sin\phi \quad . \end{aligned} \tag{2}$$

For the performed measurements the values of E_{Re} are bigger than E_{Im} which means that the gas/liquid interface of the selected solutions have a predominant viscous character.

SWCNT-TPP *mixed* have the smallest viscoelasticity value, while SWCNT-TPP *linked* has the highest values of both |*E*| and Φ. DMF values are between the values obtained for the nanotubes mixtures. The visco-elastic phase lag (Φ) results present a similar behavior.

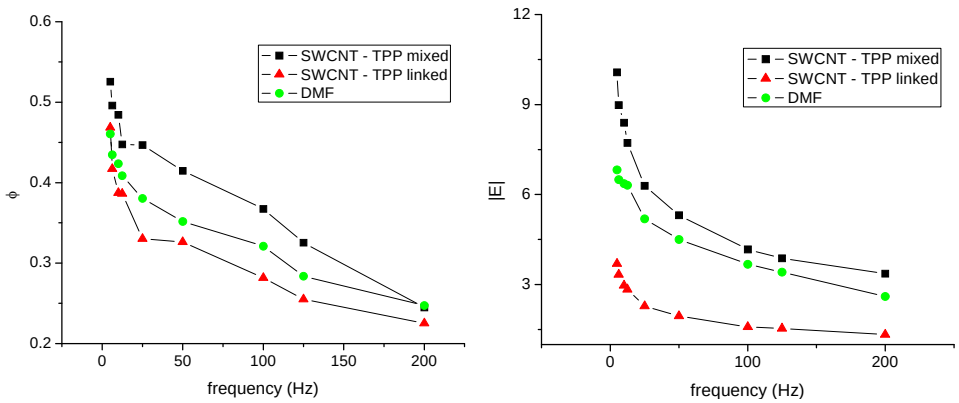

(a) (b)

Fig. 5 – Visco-elastic modulus (|*E*|) (a) and the phase lag (Φ) (b) values (online color).

For the performed measurements the values of E_{Re} are larger than E_{Im} which means that the gas/liquid interface of the studied solutions have a predominant viscous character.

The obtained differences for the SWCNT compounds highlight a viscosity and surface tension values increase due to the conjugation with the porphyrin molecules.

3.3. STUDY BY LASER INDUCED FLUORESCENCE

In Fig. 6, there are shown the LIF spectra recorded for the *linked* and *mixed* compounds. The laser pulse energy at 532 nm was 8 mJ. In the shown spectra one may observe the characteristic fluorescence emission peaks of TPP at 630 nm, 652 nm, and respectively 716 nm.

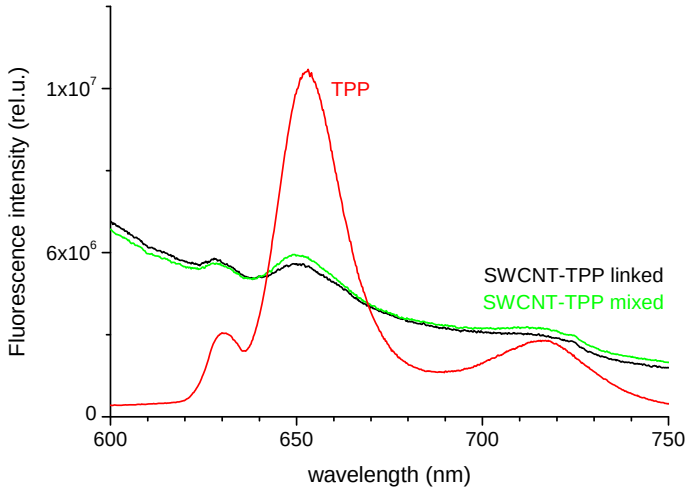

Fig. 6 – The LIF spectra for mixed and linked compounds compared with TPP spectrum (online color).

The concentration of TPP in DMF was 2×10^{-7} M corresponding to the equivalent of TPP concentration determined from absorption spectrum of the *linked* compound solution.

The smaller value of the fluorescence intensity of the *linked* compound is due to the fact that the excited linked TPP molecule transfer the energy to the SWCNT when covalently bonded and consequently less of the energy of excited TPP goes to fluorescent emission, leading to lower values of fluorescence intensity compared to that of a mixture of components. The smaller fluorescence intensity for linked compounds highlights the conjugation of TPP with SWCNT which favors the inter-molecular energy transfer.

3.4. STUDIES BY FTIR SPECTROSCOPY

In order to assess the covalent binding of TPP with SWCNT, the FTIR spectroscopy was used. The FTIR spectrum of *linked* compound was recorded and compared with the spectra of the raw components: TPP and SWCNT. Figure 7 shows the compounds spectra recorded in the 1800–500 cm^{-1} spectral range, where the carboxylation reaction and the amide bonding nanotubes-porphyrin are active.

The amino-functionalized SWCNT spectrum shows the NH_2 vibration band at 1577 cm^{-1} which disappears for the *linked* compound, this being a proof for the covalent binding.

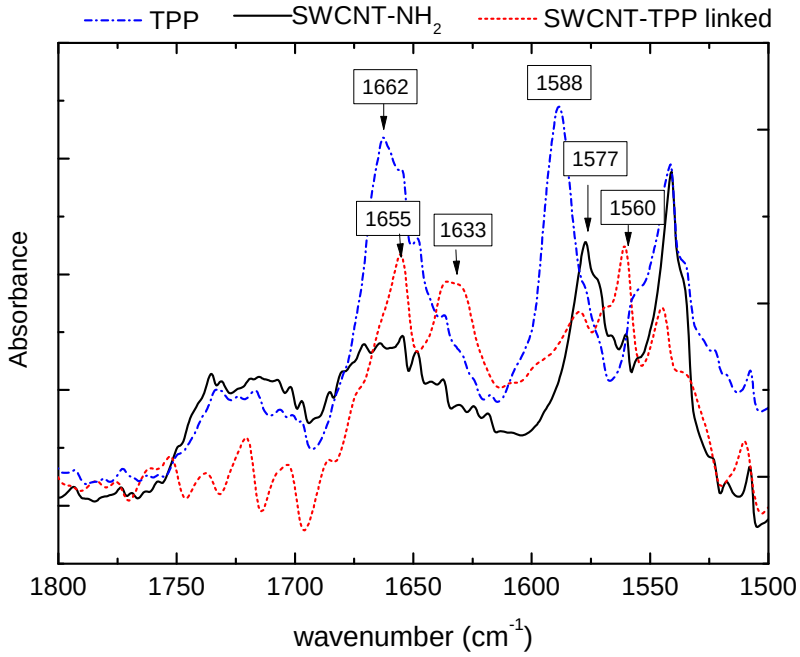

Fig. 7 – The FTIR spectra for TPP, SWCNT-NH_2, and the conjugated compound (online color).

Further, one may observe that the characteristic bands of the carbonyl moiety at 1662 cm^{-1} (stretching C = O) and 1588 cm^{-1} (vibration O-C=O), present in TPP molecule spectrum, disappear from the spectra of the conjugated product damped by conjugation.

In the mean time, the characteristic amide bands at 1633 cm^{-1} (amide I) and 1560 cm^{-1} (amide II) clearly show-up in the FTIR spectrum of the linked compound. These demonstrate the carboxylation reaction and formation of amide bonds and consequently, the achievement of the targeted conjugate compound.

4. CONCLUSIONS

This paper reports the synthesis and photophysics characterization of a compound obtained by the covalent binding of SWCNT (SWCNT-NH_2) with TPP (a photosensitizing non-metallic triphenyl porphine). The synthesized product was characterized by direct comparison of their photophysical properties with the ones of the counterparts of the building-up components.

The absorption spectra of the synthesized nano-compounds clearly display the features of both the SWCNT and the TPP compound. The linked compounds have proven to be photo-stable when irradiated with 400–800 nm band of a CW Xe lamp radiation with the power density of 145 mW/cm^2.

The obtained differences for the SWCNT compounds highlight an increase of viscosity and surface tension values due to the conjugation with the porphyrin molecules.

The fluorescence spectroscopy also highlights the conjugation of the raw compounds by synthesis, revealing a smaller value of the linked TPP fluorescence, as compared to the mixed compound, due to intermolecular energy transfer.

As an ultimate certification of the covalent linking of the amino-SWCNT with porphyrin derivative TPP, the FTIR spectra of the *linked* compounds showed typical amide-bonding bands at 1633 cm^{-1} and 1560 cm^{-1}. The FTIR spectra also reveal the disappearance of the NH_2 vibration band of the primary amino-CNT at 1577 cm^{-1} for the *linked* compound.

Acknowledgements. This work was supported by CNCS-UEFISCDI through the project number PN- PN-II-ID-PCE-2011-3-0922. Viorel Nastasa was supported by the strategic grant POSDRU/159/1.5/S/137750. This work has been made under the umbrella of the COST Actions MP1106 and MP1205.

REFERENCES

1. M. Boni, V. Nastasa, I. R. Andrei, A. Staicu, M. L. Pascu, Biomicrofluidics **9**, 014126, 2015.
2. A. Smarandache, Photomed. Laser Surg., **30**, 262–267 (2015).
3. J. Moreno-Moraga, E. Hernández, J. Royo, J. Alcolea, M.J. Isarría, M. L. Pascu, A. Smarandache, M. Trelles, Las. Med. Sci., **28**, 925–933 (2013).
4. Bianco, A., Kostarelos, K., Prato, M., Curr. Opin. Chem. Biol., **9**, 674 (2005).
5. Dhar, S., Liu, Z., Thomale, J., Dai, H., Lippard, S. J., J. Am. Chem. Soc. **130**, 11467 (2008).
6. Feazell R.P., Nakayama-Ratchford, N., Dai. H., J. Am. Chem. Soc., **129**, 8438–9 (2007).
7. Liu, Z., Chen, K., Davis, C., Sherlock, S.,Cao, Q., Chen, X., Dai, H., Cancer Res., **68**, 6652 (2008).
8. Liu, Z., Tabakman, S., Welsher, K., Dai, H., Nano Res., **2**, 85 (2009).
9. M. L. Pascu, A. Staicu, L. Voicu, M. Brezeanu, B. Carstocea, R. Pascu, D. Gazdaru, Anticancer Res., **24**, 2925 (2004).
10. M. L. Pascu, M. Brezeanu, L. Voicu, A. Staicu, B. Carstocea, R. Pascu, In vivo, **19**, 215 (2005).
11. M.L. Pascu, V. Nastasa, A. Smarandache, A. Militaru, A. Martins, M. Viveiros, M. Boni, I. Andrei, A. Pascu, A. Staicu, J. Molnar, S. Fanning, L. Amaral, Rec. Pat. Rev. Anti-Infect. Drug Discov., **6**, 147 (2011).

12. M.L. Pascu, A. Smarandache, J. Kristiansen, A. Militaru, V. Nastasa, L. Amaral, Lasers Med Sci **26**, S25 (2011).
13. M. Boni, V. Nastasa, A.Militaru, A. Smarandache, I.R. Andrei, A. Staicu, M.L. Pascu, Rom. Rep. Phys., **64**, 1179 (2012).
14. M.L. Pascu, I.R. Andrei, M. Ferrari, A. Staicu, A. Smarandache, A. Mahamoud, V. Nastasa, L. Liggieri, Colloid Surf. A-Physicochem. Eng. Asp., **365**, 83 (2010).
15. M. L. Pascu, B. Danko, A. Martins, N. Jedlinszki, T. Alexandru, V. Nastasa, M., Boni, A. Militaru, I. R. Andrei, A. Staicu, A. Hunyadi, S. Fanning, L. Amaral, PLoS ONE **8**, *2*, e55767, 2013.
16. A. Simon, T. Alexandru, M. Boni, V. Damian, A. Stoicu, V. Dutschk, M. L. Pascu, Int. J. Pharm., **475**, 270–281 (2014).
17. T. Alexandru, A. Staicu, A. Pascu, E. Radu, A. Stoicu, V. Nastasa, A. Dinache, M. Boni, L. Amaral, M. L. Pascu, J Biomed Opt, **20**, 051002 (2015).
18. M. C. Morán, T. Tozar, A. Simon, A. Dinache, A. Smarandache, I. R. Andrei, M. Boni, M.L. Pascu, F. Cirisano, M. Ferrari, Colloid Surf. B: Biointerfaces, doi: http://dx.doi.org/doi:10.1016/j.colsurfb.2015.06.041.
19. I.R. Andrei, T. Tozar, A. Dinache, M. Boni, V. Nastasa, M.L. Pascu, Eur. J. Pharm. Sci., doi: 10.1016/j.ejps.2015.09.017 (2015).
20. A. M. Armada, T. Alexandru, D. Machado, B. Danko, A. Hunyadi, A. Dinache, V. Nastasa, M. Boni, J. Ramos, M. Viveiros, J. Molnar, M. L. Pascu and L. Amaral, In vivo, **27**, 605–610 (2013).
21. W. Chidawanyika, T. Nyokong, Carbon, **48**, 2831 (2010).
22. A. Staicu, A. Pascu, M. Boni, M.L. Pascu, M. Enescu, J. Mol. Struct., **1044,** 188 (2013).
23. A. Dinache, M. Boni, T. Alexandru, E. Radu, A. Stoicu, I. Andrei, A. Staicu, L. Liggieri, V. Nastasa, M. Ferrari, M. L. Pascu, Colloid Surf. A-Physicochem. Eng., **480**, 328–335 (2015).
24. V. Nastasa, K. Samaras, Ch. Ampatzidis, T.D. Karapantsios, M.A. Trelles, J. Moreno-Moraga, A. Smarandache, M.L. Pascu, Int. J. Pharm., **478**, 588–596 (2015).